PhenoGMM: Gaussian mixture modelling of microbial cytometry data enables efficient predictions of biodiversity

Peter Rubbens [1]*, Ruben Props [2], Frederiek-Maarten Kerckhof [2], Nico Boon [2], Willem Waegeman [1]

[1]KERMIT, Department of Data Analysis and Mathematical Modelling, Ghent University, Coupure Links 653, B-9000, Gent, Belgium
[2]Center for Microbial Ecology and Technology (CMET), Ghent University, Coupure Links 653, B-9000, Gent, Belgium.

*To whom correspondence should be addressed.

Abstract

Motivation: Microbial flow cytometry allows to rapidly characterize microbial community diversity and dynamics. Recent research has demonstrated a strong connection between the cytometric diversity and taxonomic diversity based on 16S rRNA gene amplicon sequencing data. This creates the opportunity to integrate both types of data to study and predict the microbial community diversity in an automated and efficient way. However, microbial flow cytometry data results in a number of unique challenges that need to be addressed.

Results: The results of our work are threefold: i) We expand current microbial cytometry fingerprinting approaches by using a model-based fingerprinting approach based upon Gaussian Mixture Models, which we called *PhenoGMM*. ii) We show that microbial diversity can be rapidly estimated by *PhenoGMM*. In combination with a supervised machine learning model, diversity estimations based on 16S rRNA gene amplicon sequencing data can be predicted. iii) We evaluate our method extensively by using multiple datasets from different ecosystems and compare its predictive power with a generic binning fingerprinting approach that is commonly used in microbial flow cytometry. These results confirm the strong connection between the genetic make-up of a microbial community and its phenotypic properties as measured by flow cytometry.

Availability: All code and data supporting this manuscript is freely available on GitHub at: `https://github.com/prubbens/PhenoGMM`. Raw flow cytometry data is freely available on FlowRepository and raw sequences via the NCBI Sequence Read Archive. The functionality of *PhenoGMM* has been incorporated in the R package PhenoFlow: `https://github.com/CMET-UGent/Phenoflow_package`.

Contact: Peter.Rubbens@UGent.be

Supplementary information: Supplementary data are available in attachment to this submission.

1 Introduction

Life as we know it would not be possible without microorganisms (Gilbert and Neufeld, 2014). Microbial communities are driving forces of biogeochemical processes such as the carbon and nitrogen cycle (Falkowski *et al.*, 2008), they maintain human health (Young, 2017) and they are used for the creation of a vast array of products, such as chemicals, antibiotics and food (Blaser *et al.*, 2016). The field of microbial ecology is interested in the diversity of a community and its relation to ecosystem functionality (Konopka *et al.*, 2015). Various tools have been developed to study and monitor microbial communities. With the emergence of 16S rRNA gene sequencing, researchers have uncovered the genotypic diversity of microbial communities to a large extent (Van Dijk *et al.*, 2014). Although advances have been made to perform sequencing in real-time (Ardui *et al.*, 2018), most 16S rRNA gene amplicon sequencing surveys are still expensive (Sims *et al.*, 2014) and laborious in time (van Dorst *et al.*, 2014).

Instead of solely focusing on genotypic information, there is a need to combine omics data with phenotypic information (De Vrieze *et al.*, 2018). One of such tools to study the phenotypic identity of microbial communities is flow cytometry (FCM). FCM is a high-throughput technique, able to measure hundreds to thousands of individual cells in mere seconds. These measurements result in a multivariate description of each cell, derived from both scatter and fluorescence signals. The first is related to cell size and morphology, while the latter depends on either autofluorescence properties or the interaction between the cell and a specific stain. Common for microbial FCM is to use a stain that interacts with the nucleic acid content of a cell (Koch *et al.*, 2013b; Van Nevel *et al.*, 2013).

Many algorithms exist in the field of immunophenotyping cytometry to identify separated cell populations (see e.g. the extensive benchmark

studies by Aghaeepour *et al.* (2013) and Weber and Robinson (2016)). However, the number of variables that describe a bacterial cell is typically much lower than is common for cytometry setups studying mammalian cells. As a result, cytometric distributions of individual bacterial populations tend to overlap (Rubbens *et al.*, 2017a), as the number of bacterial populations in a community is typically much larger than the number of differentiating signals. Therefore, bacterial cytometry data is characterized by overlapping cell populations and these algorithms cannot be applied for the analysis bacterial cytometry data. Consequently, data analysis pipelines should be designed to address these characteristics.

In previous research, microbiologists have relied on cytometric *fingerprinting* techniques (Koch *et al.*, 2013b; Props *et al.*, 2016). The approaches that are currently used for the analysis of bacterial communities can be broadly divided in two categories: i) manual annotation of clusters (Günther *et al.*, 2012; Koch *et al.*, 2013b) and ii) automated approaches that employ binning strategies (Li, 1997; Koch *et al.*, 2013a; García *et al.*, 2015; Props *et al.*, 2016). Such a fingerprint allows to derive community-level variables in terms of the number of bins or clusters (i.e. gates), cell counts per cluster and the position of those clusters (Koch *et al.*, 2014), despite the fact that there are no or only a few clearly separated cell populations. These methods have a number of drawbacks: i) Manual gating of regions of interest is laborious in time and operator dependent, ii) only bivariate interactions of cytometry channels are considered and iii) traditional binning approaches result in a large number of variables (e.g., a fixed grid of dimensions 100×100 will result in 10,000 sample-describing variables).

After a fingerprint has been constructed, one can calculate what is called the *cytometric* or *phenotypic* diversity of a community (Li, 1997). These are estimations of the diversity of a microbial community based on the cell counts per cluster. If many clusters contain cells, a community can be considered as 'rich'. If the cells are equally distributed over those clusters, a community can be considered as 'even'. Recent reports have shown a significant correlation between the cytometric diversity and genotypic diversity derived from 16S gene sequencing data (García *et al.*, 2015; Props *et al.*, 2016, 2018). In other words, there is a strong connection between the genetic make-up of a microbial community and its phenotypic properties, which can be quantified. This result has been backed up by molecular identification using DGGE of sorted subpopulations (Park *et al.*, 2005; Koch *et al.*, 2013b), the sequencing of sorted individual cells or subpopulations (Zimmermann *et al.*, 2016; Stepanauskas *et al.*, 2017; Günther *et al.*, 2018) and by using a bottom-up approach in which individual bacterial populations resulted in unique cytometric characterizations, which can be automatically identified using machine learning models (Rubbens *et al.*, 2017a).

We propose an extension of current fingerprinting approaches that is able to deal with overlapping cell populations. Our workflow, which is called '*PhenoGMM*', makes use of Gaussian mixture models (GMM). GMMs have been successfully applied to cytometry data before to identify separated cell populations in an automated way (Boedigheimer and Ferbas, 2008; Reiter *et al.*, 2016). Interestingly, Hyrkas *et al.* (2015) have shown that their GMM approach outperformed state-of-the-art immunophenotyping cytometry algorithms for the automated identification of phytoplankton populations. By overclustering the data, GMMs can also be used to describe the distribution of the data, and therefore *PhenoGMM* is able to deal with overlapping cell populations. In addition, the number of mixtures that are needed to describe the data is much lower compared to the number of variables that result from traditional binning approaches. This facilitates the use of supervised machine learning models. We demonstrate that bacterial diversity can be predicted based on cytometric fingerprints derived from PhenoGMM. We illustrate our method using multiple datasets, in which we use diversity values derived from 16S rRNA gene amplicon sequencing data as target values that need to be predicted. We compare its performance with the predictive power of a generic traditional binning approach, which we have called *PhenoGrid*. Finally, we highlight a number of possible extensions concerning the integration of FCM with 16S rRNA gene sequencing, such as the calculation of β-diversity values, the imputation of missing diversity values and the prediction of individual OTU abundances based on FCM data.

Materials and Methods

Methodology

Preprocessing

Two steps are carried out for all measurements before further analysis of the data. First, all individual channels are transformed using $f(x) = \text{asinh}(x)$. Next, background due to debris and noise has been removed using a fixed digital gating strategy (Prest *et al.*, 2013; Props *et al.*, 2016). In other words, a single gate is applied to separate bacterial cells from background and is used for all samples.

Cytometric fingerprinting using Gaussian Mixture Models

In order to create a fingerprint template that can be used to extract variables describing a specific sample, all samples in the dataset in the training set need to be concatenated. Files are first subsampled to the same number of cells per file (`N_CELLS_MIN`), in order to not bias the Gaussian Mixture Model (GMM) towards a specific sample. This number can either be the lowest number of cells present in one sample, or a number of choice. A rough guideline can be to not let the training set be larger than 1×10^6 cells, depending on computational resources. If n denotes the total number of samples, then the total number of cells (`N_CELLS`) in the training set will be determined as $\texttt{N\_CELLS} = n \times \texttt{N\_REP} \times \texttt{N\_CELLS\_MIN}$, in which `N_REP` denotes the number of technical replicates of a specific sample. Typically, forward (FSC) and side scatter (SSC) channels are included, along with one or two targeted fluorescence channels (denoted as FL*X*, in which *X* indicates the number of a specific fluorescence detector). Unless noted otherwise, channels FSC-H, SSC-H and FL1-H (488 nm) were included for data analysis.

Once this training set is created, a GMM of K mixtures can be fitted to the data. If $\mathbf{X}$ denotes the entire datamatrix or training set containing N cells, then $\mathbf{X}$ consists of cells written as $\boldsymbol{x}_1, ..., \boldsymbol{x}_N$, of which each cell is described by D variables (i.e., the number of signals collected from the flow cytometer). Cell i is described as $\boldsymbol{x}_i = \{x_i^1, ..., x_i^D\}$. A GMM consists out of a superposition of normal distributions $\mathcal{N}$, of which each distribution has its own mean μ and covariance matrix Σ. Each mixture has a mixing coefficient or weight π, which represents the fraction of data each mixture is describing. The distribution p, which describes the GMM, can be written as follows:

$$p(\mathbf{X}) = \sum_{k=1}^{K} \pi_k \mathcal{N}(\mathbf{X}|\boldsymbol{\mu}_k, \boldsymbol{\Sigma}_k). \quad (1)$$

The set of parameters $\Theta = [\pi_k, \boldsymbol{\mu}_k, \boldsymbol{\Sigma}_k]_{k=1}^K$ is determined by the expectation-maximization (EM) algorithm (Bishop, 2006). Once a GMM has been trained on the concatenated data, one can cluster the cells in each sample separately using the trained GMM. For this step, either a specific number of cells of choice are sampled per replicate, or the lowest number of cells of the replicates that are part of that specific sample, denoted as `N_CELLS_REP`. After clustering, we count the number of cells per cluster, after which the relative number of cells per cluster and sample can be retrieved. The resulting variables can be used for different purposes: i) to calculate diversity metrics in an unsupervised way or ii) as input variables

to be included in predictive models. An illustration of *PhenoGMM* can be seen in Fig. 1.

We used the GaussianMixture() function of the scikit-learn machine learning library to implement our method (Pedregosa *et al.*, 2011). This function contains four different ways in which the covariance matrix of each mixture is determined:

- `diag`: each mixture has its own diagonal covariance matrix.
- `full`: each mixture has its own general covariance matrix.
- `spherical`: each mixture has its own single variance.[1]
- `tied`: all mixtures share the same general covariance matrix.

Unless otherwise noted, we let each mixture have its own general covariance matrix (`full`). mClust was used to integrate *PhenoGMM* in the R package PhenoFlow (Scrucca *et al.*, 2016).

Defining α- and β-diversity

Both 16S gene amplicon sequencing and flow cytometry fingerprints give rise to a compositional representation of a microbial community. The first is determined by counting the number of similar sequences at a certain taxonomic level, i.e. a taxonomic unit, the latter by counting the number of cells present in a predefined gate or cluster in the cytometric fingerprint, the phenotypic unit. Based on abundance data, one can calculate both α- and β-diversity metrics. The first quantifies the diversity within a sample, the latter the diversity between samples. As various diversity metrics exist in ecology to calculate α-diversity; we use the Hill numbers to quantify community diversity (Hill, 1973), as proposed by recent reviews of Leinster and Cobbold (2012) and Daly *et al.* (2018). If we let $\mathbf{p} = p_1, ..., p_S$ represent the vector of relative abundances, describing the abundance of S bacterial populations, then we can define the richness (D_0) and evenness (D_1, D_2) of a microbial community as follows:

$$D_{q=0}(\mathbf{p}) = S, \tag{2}$$

$$D_{q=1}(\mathbf{p}) = \exp(-\sum_{i=1}^{S} p_i \ln p_i), \tag{3}$$

$$D_{q=2}(\mathbf{p}) = \frac{1}{\sum_{i=1}^{S} p_i^2}. \tag{4}$$

q denotes the order of the Hill-number, which is part of a general family, which can be denoted as D_q^p. It expresses the weight that is given to more abundant populations.

β-diversity quantifies the difference in compositions between different samples. Typically, this is calculated by performing ordination on a dissimilarity matrix that contains the dissimilarities or distances between samples. We quantify the dissimilarity between samples using the Bray-Curtis dissimilarity (Bray and Curtis, 1957). If we let BC_{AB} denote the dissimilarity between samples A and B, BC_{AB} is calculated using the following equation:

$$BC_{AB} = \frac{\sum_{i=1}^{S} |p_{A,i} - p_{B,i}|}{\sum_{i=1}^{S} |p_{A,i} + p_{B,i}|} \tag{5}$$

Predictive modeling

FCM fingerprints can be used as input variables to train a machine learning model. We used Random Forest regression (Breiman, 2001), an ensemble of decision trees, to predict α-diversity metrics. A randomized grid search was performed to search for an optimal hyperparameter combination (Bergstra and Bengio, 2012). This means that a 100 random combinations of hyperparameter values were evaluated. The maximum number of variables that are considered at an individual split for a decision tree was randomly drawn from $\{1, ..., K\}$, the minimum number of samples for a specific leaf was randomly drawn between $\{1, ..., 5\}$. The cross-validation strategy differed per experiment, and is described accordingly.

[1] Note, this is not the same as k-means clustering. In this case, all mixtures would share the same single variance.

Datasets

Dataset 1: In Silico Bacterial Communities

Data from 20 individual bacterial populations that were measured through FCM were collected from Rubbens *et al.* (2017a). The data is available at FlowRepository (accession ID: FR-FCM-ZZSH). In brief, bacterial populations were measured after 24h of incubation, stained with SYBR Green I and two technical replicates per population were measured on an Accuri C6 (BD Biosciences). Fluorescence was measured by the targeted detector (FL1, 530/30 nm) and three additional detectors, next to forward (FSC) and side scatter (SSH) information that was collected as well. Additional automated denoising was performed using the FlowAI package (v1.4.4., default settings, target channel: FL1, changepoint detection: 150, Monaco *et al.* (2016)). A full experimental overview can be found in Rubbens *et al.* (2017a). The lowest number of cells collected after background removal amounted to 13166 cells.

Dataset 2: Cooling water microbiome

Data was used as presented in Props *et al.* (2016). Samples were collected from the cooling water of a discontinuously operated research nuclear reactor. This reactor underwent four phases: control, startup, operational and shutdown. Samples were taken from two surveys (Survey I and II) and analyzed through 16S rRNA gene amplicon sequencing ($n = 77$) and FCM ($n = 153$). The sequencing and flow cytometric procedures are extensively described in Props *et al.* (2016). Taxonomic identification of the microbial communities was done at the operational taxonomic unit (OTU) level at 97% similarity. Sequences are available from the NCBI Sequence Read Archive (SRA) under (accession ID: SRP066190), flow cytometry data is available from FlowRepository (accession ID: FR-FCM-ZZNA). The lowest number of cells collected after background removal amounted to 10565 cells.

Dataset 3: Freshwater lake system microbiome

A total of 173 samples collected from three types of freshwater lake systems were analyzed. Data were used as presented in (Rubbens *et al.*, 2019). All samples were analyzed through 16S rRNA gene amplicon sequencing and FCM. Samples originate from three different freshwater lake systems: (1) 49 samples from Lake Michigan (2013 & 2015), (2) 62 samples from Muskegon Lake (2013-2015; one of Lake Michigan's estuaries), and (3) 62 samples from twelve Inland lakes in Southeastern Michigan (2014-2015). Field sampling, DNA extraction, DNA sequencing and processing are described in Chiang *et al.* (2018). Fastq files were submitted to NCBI SRA under BioProject accession number PRJNA412984 and PRJNA414423. Taxonomic identification of microbial communities was done for each of the three lake datasets separately and treated with an OTU abundance threshold cutoff of either 1 sequence in 3% of the samples. For comparison of taxonomic abundances across samples, each the three datasets were then rarefied to an even sequencing depth, which was 4,491 sequences for Muskegon Lake samples, 5,724 sequences for the Lake Michigan samples, and 9,037 sequences for the Inland lake samples. Next, the relative abundance at the OTU level was calculated by taking the count value and dividing it by the sequencing depth of the sample. Flow cytometry procedures are extensively described in Props *et al.* (2018). In brief, samples were stained with SYBR Green I and three technical replicates were measured on an

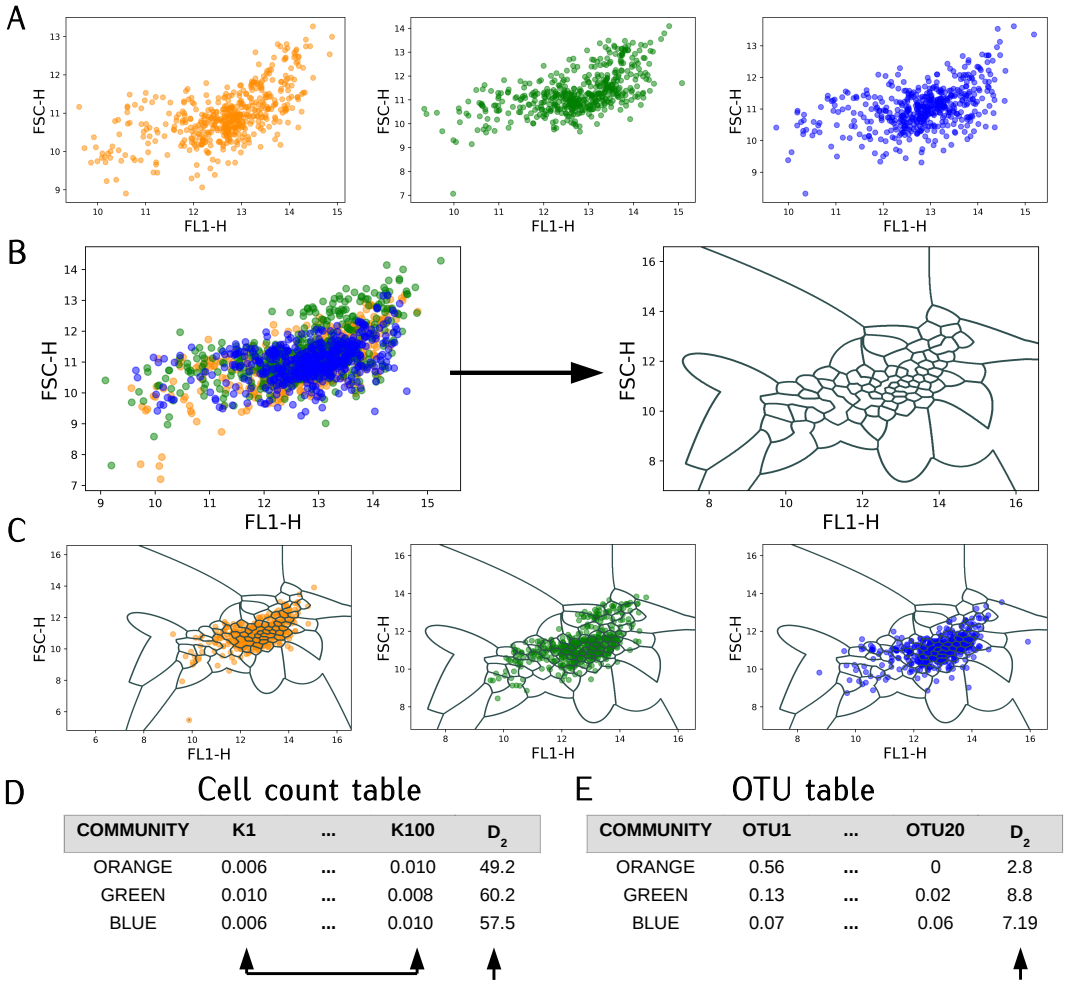

COMMUNITY	K1	...	K100	D_2
ORANGE	0.006	...	0.010	49.2
GREEN	0.010	...	0.008	60.2
BLUE	0.006	...	0.010	57.5

COMMUNITY	OTU1	...	OTU20	D_2
ORANGE	0.56	...	0	2.8
GREEN	0.13	...	0.02	8.8
BLUE	0.07	...	0.06	7.19

Fig. 1. Illustration of PhenoGMM for two channels (FL1-H and FSC-H) using $K = 100$ mixtures. A: The analysis starts from cytometric measurements of three bacterial communities of interest, noted as 'ORANGE' ($S = 6$), 'GREEN' ($S = 8$) and 'BLUE' ($S = 15$). B: Data of the three communities are concatenated into one dataframe, to which is a GMM with $K = 100$ mixtures is fitted. This results in a cluster structure, which is depicted on the right. C: The fingerprint template is used to derive relative cell counts per cluster and per bacterial community. D: This results in a 'count' table, which can be used to rapidly quantify the cytometric diversity based on equations 2-4 (in this case D_2). E: Based on the count table derived using PhenoGMM, one can try and predict diversity metrics based another type of data such as 16S rRNA gene sequencing, using a machine learning model.

Accuri C6 (BD Biosciences). The lowest number of cells collected after denoising amounted to 2342 cells.

Experimental setup

Our proposed fingerprinting approach based on GMMs was compared to a generic fixed binning approach, which we have called *PhenoGrid*. In brief, we implemented a binning grid of $L = 128 \times 128$ for each bivariate parameter combination, after which relative cell fractions per bin were determined. The resulting cell fractions were next concatenated into one vector.

Both *PhenoGMM* and *PhenoGrid* result in multiple variables that describe cell counts, either per cluster or bin. This can be used to perform:

1. Unsupervised α-diversity estimation, by directly calculating D_0, D_1 and D_2 according to equations 2, 3 and 4 based on the cell count vectors.
2. Unsupervised β-diversity estimations, by calculating Bray-Curtis dissimilarities (equation 5) between the cytometric fingerprints.
3. Supervised α-diversity predictions, with cytometric fingerprints as input variables to predict true target variables D_0, D_1 and D_2 based on 16S rRNA gene sequencing data, by means of Random Forest regression.
4. Supervised taxon abundance predictions, with cytometric fingerprints as input variables to predict true taxon abundances, based on 16S rRNA gene sequencing data, by means of Random Forest regression.

Research question 1: Does *PhenoGMM* allow α-diversity estimations of *in silico* synthetic microbial communities?

The main goal is to estimate (i.e., unsupervised) or predict (i.e., supervised) α-diversity metrics based on cytometric fingerprinting of the data. Dataset 1 contains the cytometric characterization of individual bacterial populations. By using a data-aggregation step, it is possible to create bacterial communities of different compositions. As it is known which cell belongs to which species, diversity indices can be calculated with high accuracy by simply counting the number of bacterial populations that are present in a community (D_0) or by counting the fraction of cells that comes from every population (D_1, D_2). A training set representing 300

different *in silico* compositions, and a test set containing 100 different compositions, were created in the following way:

1. Sample uniformly at random a number S_i' between two and 20; this is the number of populations that will make up community i.
2. Select randomly which S_i' populations will make up the total community (from $S = 20$ populations).
3. Use the Dirichlet distribution to randomly sample a specific composition that sums to 1, containing the selected populations. The Dirichlet distribution can be used to model the joint distribution of individual fractions of multiple species (Friedman and Alm, 2012). The evenness of the composition depends on the concentration parameter a, which determines how evenly the weight will be spread over multiple species. If a is low, only a few species will make up a large part of the community. If a is high, the fraction of each population will be almost equally divided.

Using these compositions, *in silico* communities can be sampled accordingly. This results in a training and test set containing 300 and 100 cytometric representations of bacterial communities respectively, ranging from two to 20 populations, with varying compositions. This experiment was repeated for $a = 0.1, 1, 10$. Random forests were trained using 5-fold cross-validation. Both unsupervised and supervised α-diversity estimations were reported for the test set.

Research question 2: Does *PhenoGMM* allow α-diversity predictions based on 16S rRNA gene sequencing data for freshwater microbial communities?

Analogous to experiment 1, the main goal is here to both estimate and predict α-diversity metrics based on cytometric fingerprinting of the data. However, different from dataset 1, we will now use α-diversity values based on 16S rRNA gene amplicon sequencing. Dataset 2 and 3 contain natural communities, which were measured both by FCM and 16S rRNA gene amplicon sequencing. These values were used as target variables to predict. 10-fold cross-validation was used to select hyperparameters for the Random Forest model, for which predictive performance of the validation sets is reported. Unsupervised estimations were reported based on the full dataset.

Extensions

1. We quantified the correlation between β-diversity estimations based on FCM and 16S rRNA gene amplicon sequencing data for all datasets.
2. Missing diversity values based on 16S rRNA gene amplicon sequencing were imputed based on *PhenoGMM* for dataset 2.
3. Individual abundances of the first twenty bacterial populations in the composition (either sampled *in silico* or based on 16S rRNA gene sequencing) were predicted based on cytometric fingerprints for all datasets.

Performance evaluation

- Unsupervised and supervised α-diversity estimations were quantified by calculating the Kendall's rank correlation coefficient τ between the true and estimated values. The τ_B implementation, which is able to deal with ties, is calculated as follows:

$$\tau_B = \frac{N_c - N_d}{\sqrt{(N_c + N_d + N_t) \times (N_c + N_d + N_u)}}. \quad (6)$$

  N_c denotes the number of concordant pairs between true and predicted values, N_d the number of discordant pairs, N_t the number of ties in the true values and N_u the number of ties in the predicted values. Values range from -1 (perfect negative association) to +1 (perfect positive association) and a value of 0 indicates the absence of an association. This was done using the kendalltau() function in Scipy (v1.0.0).
- Supervised predictions are evaluated by calculating the R^2 between true ($\mathbf{y} = \{y_1, ..., y_n\}$) and predicted ($\hat{\mathbf{y}} = \{\hat{y}_1, ..., \hat{y}_n\}$) values:

$$R^2(\mathbf{y}, \hat{\mathbf{y}}) = 1 - \frac{\sum_{i=0}^{n-1}(y_i - \hat{y}_i)^2}{\sum_{i=0}^{n-1}(y_i - \bar{y})^2}, \quad (7)$$

  in which $\bar{y}$ denotes the average value of $\mathbf{y}$. If $R^2 = 1$, predictions were correctly estimated. If $R^2 < 0$, predictions are worse than random guessing.The r2_score()-function from the scikit-learn machine learning library was used.
- Unsupervised β-diversity estimations were evaluated by calculating the correlation between Bray-Curtis dissimilarity matrices (BC) based on FCM and 16S rRNA gene sequencing data using a Mantel-test (Mantel, 1967). This test assesses the alternative hypothesis that the distances between samples based on cytometry data are linearly correlated with those based on 16S rRNA gene sequencing data. It makes use of the cross-product term Z_M across the two matrices for each element ij:

$$Z_M = \sum_{i=1}^{n}\sum_{j=1}^{n} BC_{ij}^{\text{FCM}} \times BC_{ij}^{\text{16S}}. \quad (8)$$

  The test statistic Z_M is normalized and then compared to a null distribution, based on 1000 permutations.

Results

PhenoGMM allows to predict α-diversity of *in silico* synthetic microbial communities

300 different bacterial communities were assembled by aggregating cytometric characterizations of individual populations in varying compositions (creating communities *in silico*), constituting the training set. This allowed to simulate community compositions in an accurate way, as cell labels according to taxonomy are known for every individual cell. Based on these compositions, diversity metrics could be accurately determined, and were used as target variables to evaluate diversity estimations and predictions. We repeated the experiment for three different values of a, in which a determines how evenly the weight is spread amongst the different populations. If a is small, only a few species will be dominantly present, if a is large, chances are high that the weight is evenly spread amongst the different populations. This is illustrated using Lorenz curves, which depict the cumulative proportion of abundance versus the cumulative proportion of bacterial species (SI Fig. 1). 100 additional bacterial communities were assembled using the same aggregation strategy, making up the test set.

Cytometric fingerprints were determined on the concatenated representation of the samples in the training set, to which a GMM of $K = 128$ or a fixed binning grid of dimensions 128×128 was fitted. The resulting cell counts were first used to directly calculate estimations of α-diversity metrics according to equations 2-4, i.e. in an unsupervised way. Second, the cell counts were used as input variables to predict D_0, D_1 and D_2 by means of Random Forest regression.

PhenoGMM was compared with a generic fixed binning approach called '*PhenoGrid*' (Table 1). To compare supervised with unsupervised performances, Kendall's τ_B was calculated between true and estimated diversity values, which also allowed to quantify the level of significance. We conclude that α-diversity could be estimated properly, as predictions were significantly correlated with the true values according to τ_B. As

Table 1. Summary of unsupervised and supervised α-diversity estimations for different a, quantified by τ_B, using both PhenoGMM versus PhenoGrid. Values denote the average τ_B after 10 runs, along with corresponding standard deviation (SD). Values are bolded if the mean value of one approach is significantly higher than the mean value of the other approach according to a student's t-test ($\alpha = 0.05$).

		PhenoGMM			*PhenoGrid*		
	Dataset	$\tau_B(D_0)$	$\tau_B(D_1)$	$\tau_B(D_2)$	$\tau_B(D_0)$	$\tau_B(D_1)$	$\tau_B(D_2)$
Unsupervised	$a = 0.1$	**0.29 ± 0.07**	**0.43 ± 0.06**	**0.40 ± 0.05**	NS	0.18 ± 0.07	NS
	$a = 1$	**0.31 ± 0.07**	**0.47 ± 0.05**	**0.47 ± 0.06**	0.23 ± 0.06	0.20 ± 0.05	0.17 ± 0.06
	$a = 10$	**0.26 ± 0.05**	**0.46 ± 0.05**	**0.45 ± 0.06**	0.20 ± 0.06	0.17 ± 0.07	NS
Supervised	$a = 0.1$	0.43 ± 0.05	**0.62 ± 0.04**	**0.62 ± 0.03**	**0.54 ± 0.03**	0.58 ± 0.02	0.54 ± 0.02
	$a = 1$	0.61 ± 0.02	0.64 ± 0.02	0.62 ± 0.04	**0.71 ± 0.03**	**0.67 ± 0.03**	0.63 ± 0.04
	$a = 10$	0.72 ± 0.04	0.71 ± 0.03	0.70 ± 0.03	0.74 ± 0.05	0.72 ± 0.04	0.72 ± 0.04

NS: Not significant (average $P > 0.05$)

expected, unsupervised estimations resulted in lower correlations with true diversity metrics compared to supervised predictions, although still significant in most cases (Kendall's τ_B, level of significance $\alpha = 0.05$). The only exceptions were D_1 and D_2 for $a = 10$ when using *PhenoGrid*. *PhenoGMM* resulted in better unsupervised α-diversity estimations than *PhenoGrid*, but both approaches resulted in a comparable supervised performance. R^2 values were considerably higher than zero, and slightly in favor of *PhenoGMM* (SI Table 1). We note that the predictive performance mainly depended on a and the diversity metric of choice. For example, the hardest setting was the one in which $a = 0.1$ and D_0 the target variable to predict. In this case only a few populations made up a large part of the community (low a), but an equal weight is attributed to all species when defining diversity. Generally, if the abundance of populations is taken into account ($q > 0$), α-diversity predictions were better. In other words, FCM is able to capture community structure rather than the identity of the community.

Computational efficiency

We timed different steps in the workflow of *PhenoGMM* for $a = 1$ and D_1. The time in seconds was determined in function of the number of mixtures K (Fig. 2A). Each analysis was run on a separate node of a computer infrastructure, with 2.6 Ghz CPU and 20GB of RAM for each node. The timing consists out of the following steps: fitting a GMM, using this model to extract variables per sample and calculating D_1 directly according to equation 3 (Fig. 2A), or with the addition of fitting a Random Forest model to predict D_1 (Fig. 2B). We sampled 5000 cells per sample. As we have 300 samples in our training set, this amounts to fitting a GMM to 1,5 million cells. Most importantly, the entire analysis remains under one hour. Most of the time is spent on fitting the GMM. Training a Random Forest model on the fitted GMM comes with an average increase of 24,4% of the runtime for $K = 256$. The predictive performance of both *PhenoGMM* and *PhenoGrid* was evaluated in function of the total runtime, indicating that *PhenoGMM* needs much less time than *PhenoGrid* to reach its optimal performance (SI Fig. 2).

Influence of hyperparameters on α-diversity estimations

In order to provide guidance concerning use of the model, the most important parameters were varied one by one (i.e., the number of included detectors D, the number of mixtures K, the number of cells sampled per file to fit a GMM denoted as N_CELLS_MIN, the number of cells sampled per individual sample to determine the cell counts per cluster denoted as N_CELLS_REP, a learning curve in function of N_SAMPLES and the TYPE of covariance matrix used to fit a GMM). The performance was quantified using $R^2(D_1)$ for $a = 1$ for a supervised analysis (SI Fig. 3). The results indicate that considering the predictive performance:

- D: including additional detectors improves the performance.
- K: generally, the higher K, the better the performance, which saturates after a specific threshold.
- N_CELLS_MIN: predictions are quite robust for this parameter.
- N_CELLS_REP: predictions are quite robust for this parameter.
- N_SAMPLES: predictive performance did not saturate yet at N_SAMPLES = 300.
- TYPE: predictions are quite robust for the type of covariance matrix, but the 'full' type resulted in the best predictions.

PhenoGMM allows to predict α-diversity for freshwater microbial communities

α-diversity predictions were made based on cytometric fingerprinting of natural microbial communities, which were either part of a cooling water system (i.e. Survey I, II or combined), or a freshwater lake system (i.e. Inland, Michigan, Muskegon or all of them combined). α-diversity values, based on 16S rRNA gene amplicon sequencing, were used as target variables to predict. Supervised predictions were the result of Random Forest regression, which was tuned using ten-fold cross-validation. Values are reported for the model that returned the best combined predictions on the validation folds using Kendall's τ_B (Table 2) and R^2_{CV} (SI Table 2). Diversity predictions were feasible (i.e., significant according to τ_B for $\alpha = 0.05$ and considerably higher than zero for R^2_{CV}), but depending on the dataset and diversity index. For example, predictions of D_0 were easier to make compared to D_1 or D_2 for the Inland lake-system and were better for the cooling water system than for the lake systems. The predictive performance of *PhenoGMM* ($K = 256$) was better or similar compared to *PhenoGrid* ($K = 128 \times 128$).

Unsupervised diversity estimations were evaluated as well (SI Table 3). Diversity estimations were highly significant for the cooling water microbiome, but were insignificant in a number of cases for the freshwater lake systems according to both approaches (D_0 and D_2 for the Inland lakes and Muskegon lake; Kendall's τ_B, $\alpha = 0.05$). *PhenoGrid* outperformed *PhenoGMM* in most cases, indicating that even more mixtures might be needed to make it competitive with *PhenoGrid* in this setting. We conclude that FCM shows a strong connection with 16S rRNA gene sequencing data. FCM is sensitive for the community structure and can be used to adequately perform microbial diversity estimations and predictions of natural communities.

***PhenoGMM* allows estimations of β-diversity**

β-diversity, which quantifies the difference in community composition between different samples, can be determined as well using both 16S rRNA gene amplicon sequencing and FCM. This was done by calculating Bray-Curtis dissimilarities between all communities based on relative fractions per OTU or mixture. A mantel test was used to calculate the correlation between Bray-Curtis dissimilarity matrices, derived from the the two types of data using both *PhenoGMM* and *PhenoGrid* (SI Table 4).

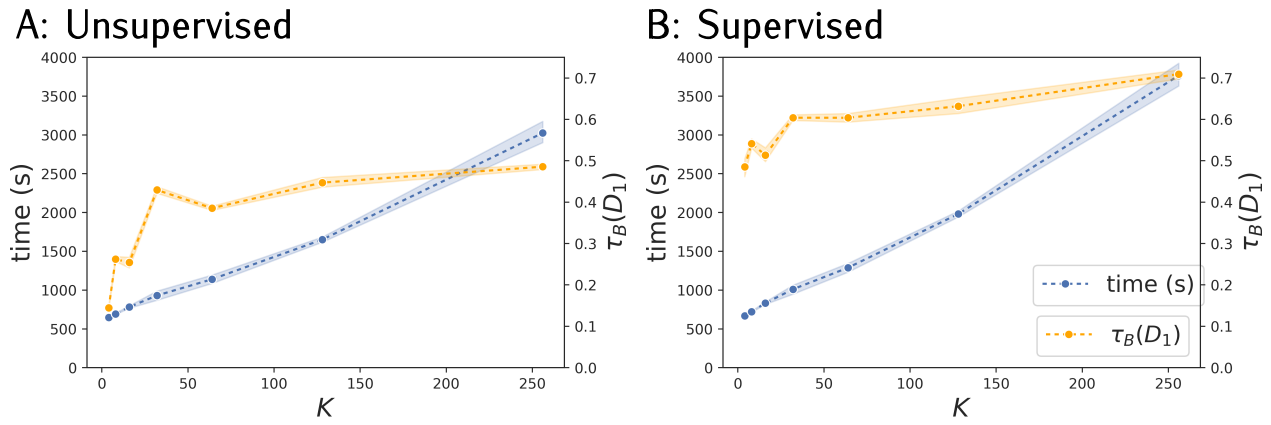

Fig. 2. Benchmarking of PhenoGMM vs PhenoGrid. Each model was run five times. A: time t, in seconds, versus K, the number of mixtures or dimension of the grid. B: Performance expressed in $R^2(D_1)$ in function of K.

Both approaches resulted in statistically significant correlations (Mantel test, $\alpha = 0.05$). *PhenoGMM* resulted in better (synthetic microbial communities) or similar (freshwater communities) β-diversity estimations compared to *PhenoGrid*.

***PhenoGMM* can be used to impute missing α-diversity values**

It is common practice in the field of microbial ecology to analyze only a subset of samples by 16S rRNA gene amplicon sequencing. This was also the case for the cooling water dataset, for which all samples ($n = 153$) were analyzed through FC<, but additionally roughly half ($n = 77$) by both FCM and 16S rRNA gene amplicon sequencing. *PhenoGMM* allowed to make inference concerning the α-diversity of these missing samples. An example is given for D_1, for both survey I and II (Fig. 3). Predictions are the average of ten runs of *PhenoGMM*. This illustrates how FCM can be integrated with 16S rRNA gene sequencing in order to frequently monitor a microbial community of interest, and reduce the number of samples that have to be analyzed by 16S rRNA gene sequencing at the same time.

***PhenoGMM* allows to predict individual bacterial abundances**

The fact that biodiversity can be estimated from cytometric data implies that the taxonomic structure of a microbial community is captured by the cytometric fingerprint. This opens up the opportunity to predict variations in abundance of individual bacterial populations as well. First, we constructed a fingerprint using 20 mixtures for the *in silico* dataset and correlated the relative cell counts per mixture with variations in individual abundances of bacterial populations (Fig. 4A). In most cases multiple clusters are correlated with multiple populations, which is due to the fact that bacterial populations exhibit overlapping cytometric fingerprints (Fig. 4B). At the same time, no cluster is correlated with all bacterial populations, motivating that despite the overlapping structure in a cytometric fingerprint, variations in the clusters can be related to variations in individual populations as well. The same procedure was applied for the Muskegon dataset, in which counts in 128 mixtures were correlated with the first 128 OTUs in the abundance table (SI Fig. 4). The same results hold, meaning that almost every OTU shows a significant correspondence with cell count variations in multiple, but never all clusters.

Therefore, we tested whether we could predict the abundance of individual bacterial populations for all datasets (Fig. 4C). For dataset 1, the individual abundances are known due to the experimental setup, for dataset 2 and 3 we tested whether we could predict abundance values for the first 20 taxa in the OTU-table based on 16S rRNA gene amplicon sequencing data[2]. Predictions of taxon abundances were quantified in terms of the R^2 on the test set for *in silico* synthetic communities or the R^2_{CV} for natural communities (Fig.4). The results indicate that individual taxon abundances can be predicted based on cytometry data. For dataset 1 this was possible for all populations, with $a = 0.1$ being the easiest setup to do so and $a = 10$ being the hardest setup to do so. This can be explained, as the weights of a composition will be divided over few species for $a = 0.1$, compared to compositions for $a = 10$. In other words, differences between individual abundances will be larger for $a = 0.1$, making it easier to predict them.

[2] Except for Survey I, for which results are presented for 18 taxa due to the fact that two taxa did not vary in abundance which resulted in 'perfect' predictions

Table 2. Summary of supervised α-diversity estimations for different a, quantified by τ_B, using both PhenoGMM versus PhenoGrid. Performance was quantified based on estimations for the validation folds, using 10-fold cross-validation. Values denote the average τ_B of 10 different runs, along with corresponding standard deviation (SE). Values are bolded if the mean value of one approach is significantly higher than the mean value of the other approach according to a student's t-test ($\alpha = 0.05$).

	PhenoGMM			*PhenoGrid*		
Dataset	$\tau_B(D_0)$	$\tau_B(D_1)$	$\tau_B(D_2)$	$\tau_B(D_0)$	$\tau_B(D_1)$	$\tau_B(D_2)$
Survey I	**0.40 ± 0.03**	0.49 ± 0.06	0.53 ± 0.05	0.27 ± 0.07	0.48 ± 0.04	0.49 ± 0.06
Survey II	**0.66 ± 0.04**	0.61 ± 0.04	0.62 ± 0.03	0.62 ± 0.03	0.59 ± 0.04	0.59 ± 0.04
Survey I+II	**0.55 ± 0.03**	**0.63 ± 0.014**	0.64 ± 0.04	0.52 ± 0.04	0.59 ± 0.03	0.61 ± 0.04
Inland	0.25 ± 0.07	**0.33 ± 0.05**	**0.22 ± 0.02**	NS	0.27 ± 0.04	NS
Michigan	**0.26 ± 0.07**	**0.42 ± 0.05**	0.39 ± 0.05	NS	0.35 ± 0.06	0.36 ± 0.03
Muskegon	**0.35 ± 0.04**	**0.29 ± 0.04**	**0.19 ± 0.08**	NS	NS	NS
All lake systems	**0.510 ± 0.018**	**0.48 ± 0.02**	**0.44 ± 0.02**	0.38 ± 0.03	0.38 ± 0.02	0.34 ± 0.03

NS: Not significant (average $P > 0.05$)

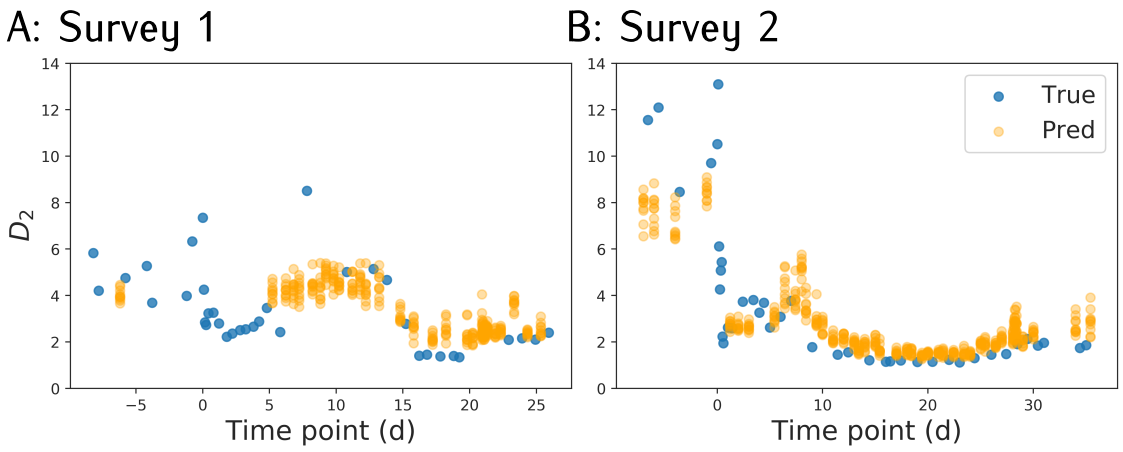

Fig. 3. Predictions of ten different runs for D_2 for which no 16S rRNA gene amplicon sequencing data was available for the cooling water dataset (Survey I and II), using PhenoGMM.

For natural communities, we note that it was possible to predict taxon abundances for 67-95% of the evaluated taxa.

Discussion

In this paper we have extensively shown that flow cytometry (FCM) can be used to estimate and predict microbial biodiversity. To do so, we proposed a more advanced fingerprinting strategy based on Gaussian Mixture Models (GMMs), called *PhenoGMM*. Our approach allows to create meaningful variables and reduces the number sample-describing variables considerably compared to traditional binning approaches. This makes the use of predictive models, in this study by means of Random Forest regression, much more feasible. We evaluated the performance of *PhenoGMM* both for unsupervised estimations and supervised predictions of biodiversity using multiple datasets. We compared it with the performance of a generic traditional binning approach, which we in this work called *PhenoGrid*.

In the first part of the paper, we constructed communities *in silico* by aggregating cytometric characterizations of individual bacterial populations in different compositions. This allowed us to simulate microbial community compositions in a highly precise and controlled way. In the second part we showed that flow cytometry data can be used to predict biodiversity values based on 16S rRNA gene sequencing data. Upon making predictions, *PhenoGMM* resulted in either more or equally accurate predictions compared to *PhenoGrid* for all datasets. Unsupervised estimations of α-diversity resulted in higher correlations with the target diversity values for *PhenoGMM* for the synthetic communities, while estimations were better for *PhenoGrid* for natural communities, for which the diversity was determined based on 16S rRNA gene amplicon sequencing. Total analysis time of *PhenoGMM* remains under one hour.

Many algorithms exist for the analysis of cytometry data. However, most of these methods are developed for an automated analysis of immunophenotyping data, in which many separated cell populations can be identified. Microbial cytometry data has a number of different characteristics, which is why most of these approaches are not applicable. The reason is that bacterial cells are typically much smaller in both cell size and volume compared to eukaryotic ells (Robinson, 2018). In addition, no general antibody-based panels have been established for microbial cells due to the high complexity of microbial communities (Koch and Müller, 2018). One has to rely on general DNA stains, for which it is difficult to develop multicolor approaches (Buysschaert *et al.*, 2016). Therefore, the number of variables describing an individual bacterial cell is typically much lower than e.g. a human cell. As a result, cytometric distributions of bacterial populations tend to overlap, as the number of bacterial populations is larger than the number of differentiating signals. GMMs allow to model overlapping cell distributions. However, as distributions overlap, it is hard to determine the exact number of populations. That is why we overcluster the data by choosing a sufficient number of K mixtures. As K increases, the performance saturates gradually, and more mixtures will not improve predictions.

Few reports exist that quantitatively evaluate fingerprinting approaches for the analysis of microbial data. A brief comparison study with $n = 21$ samples has been recently conducted (Menyhárt *et al.*, 2018), illustrating a better performance for *FlowFP* (Rogers and Holyst, 2009), compared to the use of *FlowCyBar* (Koch *et al.*, 2013b). *FlowFP* is quite similar compared to *PhenoGMM*, as it makes use of an adaptive binning approach, in which bins are smaller when the density of the data is higher, while *FlowCyBar* makes use of manually annotated clusters. However, the bins are still rectangular in shape, while *PhenoGMM* allows clusters to be of any shape. Most fingerprinting strategies make use of manual annotation of clusters or of fixed binning approaches (see e.g. the report by Koch *et al.* (2014) which qualitatively discusses different existing methods). In almost all cases, only bivariate interactions are inspected. *PhenoGMM* allows to model the full parameter space at once. This is interesting, because although it is hard to develop multicolor approaches for bacterial analyses, they are possible (see e.g. the work by Barbesti *et al.* (2000)). In addition our research group has established that additional detectors that capture signals due to spillover can assist in the discrimination between bacterial species (Rubbens *et al.*, 2017b). Therefore, the parameter space in which bacterial cells can be described is increasing, and *PhenoGMM* is able to model this straightforwardly. Because it is in an adaptive strategy as well, by defining small clusters in regions of high density and vice versa, it reduces the number of sample-describing variables considerably compared to fixed binning approaches. Other adaptive binning strategies have been proposed for microbial FCM data as well, however these still only investigate bivariate interactions (Amalfitano *et al.*, 2018; Huang *et al.*, 2018).

Our approach comes with a number of caveats. First, *PhenoGMM* fits a fingerprint template based on the concatenation of measured samples. New samples are characterized based on this template. In case multiple samples diverge considerably from those which were used to determine the template (for example in case an experiment was conducted in different conditions), we recommend to refit the model. Second, *PhenoGMM* overclusters the data, which might result in a number of correlated

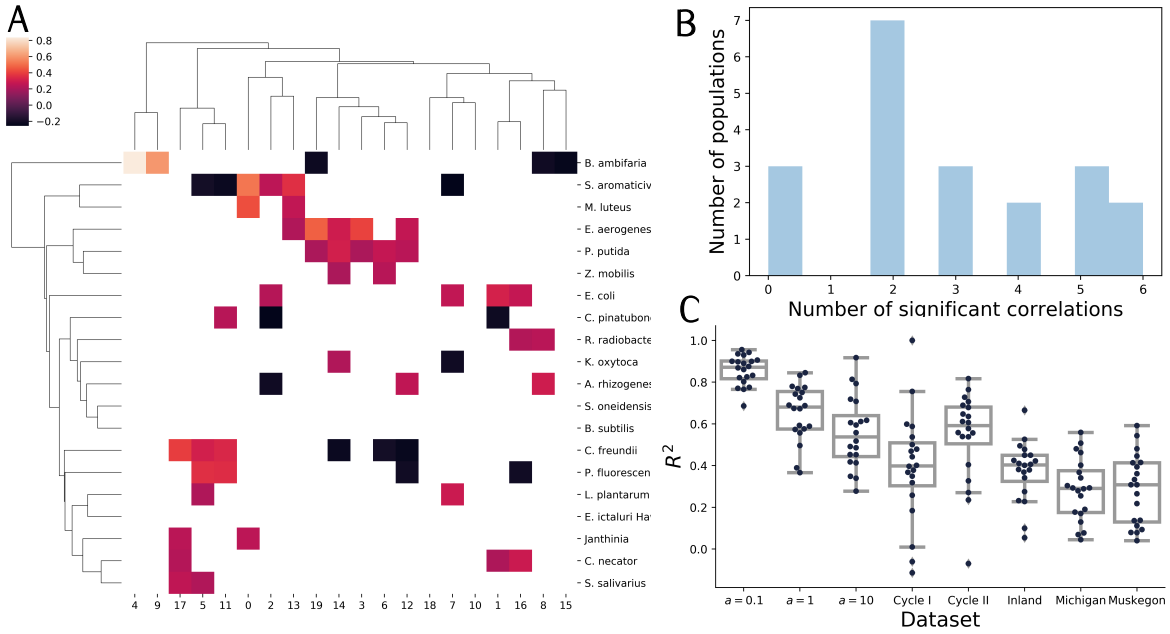

Fig. 4. A: Correspondence between variations in cell counts per mixture (columns) and abundances of bacterial populations (columns), quantified using the Kendall's τ_B. Values are given if $P \leq 0.05$, after performing a Benjamini-Hochberg correction for multiple hypothesis testing. B: Distribution of the number significant correlation with every mixture for each bacterial population. C:Predictions of taxon abundances for different datasets, expressed in terms of the R^2 for the in silico datasets, using held-out test set, for the freshwater datasets the R^2_{CV} is reported.

variables. We recommend therefore researchers to use a classification or regression method that is able to deal with multicollinearity, which is why we used Random Forest regression in this work. Other methods that might be suitable are regularized regression methods, such as the Lasso or ElasticNet (Tibshirani, 1996; Zou and Hastie, 2005). Third, although the performance tends to saturate once K is high enough, this threshold seems to application dependent, and one needs to validate the settings of the approach.

Our *in silico* benchmark study made use of cytometric characterizations of individual bacterial populations. These populations are known to exhibit considerable heterogeneity due to cell size diversity and cell cycle variations (Vives-Rego *et al.*, 2003). Our research group has recently shown that the cytometric diversity of an individual population reduces when that population is part of a co-culture (Heyse *et al.*, 2019). Therefore, data used for the *in silico* community creation setup cannot be used to study environmental samples, as we hypothesize that members of natural communities will have a different cytometric fingerprint as opposed to populations that were grown and measured individually. Yet we believe that our *in silico* approach is useful, as it allows to simulate variations in cytometric community structure with high precision.

In this study we focused mainly on estimations of α-diversity (i.e., within-sample diversity), but quantification of β-diversity (i.e. between-sample diversity) can be successfully performed as well. In addition, it is possible to predict variations in the abundance of a specific bacterial populations. This might be interesting for certain biotechnological applications, in which researchers or engineers are not interested in the total diversity of the community but in the behavior of a specific bacterial population.

PhenoGMM allows to infer diversity metrics efficiently, both in an unsupervised and supervised setting. Technological advancements have enabled an automation of the data acquisition, resulting in a detailed characterization of the microbial community on-line (i.e., samples are measured at routine intervals between 5-15 min) or even in real-time (i.e., near-continuous measurements) (Hammes *et al.*, 2012; Besmer and Hammes, 2016). Therefore we see great potential to use FCM as a monitor technique to rapidly investigate microbial community dynamics. In this work we have confirmed the strong correspondence between FCM and the genetic make-up of a community, quantified by 16S rRNA gene sequencing. Therefore, FCM can be integrated with other types of data and machine learning models can be used to exploit the relationship between the two. One fruitful approach would be to routinely monitor the microbial community using FCM, and additionally analyze states 'of high interest' by for example 16S rRNA gene amplicon sequencing. Cytometric fingerprinting in combination with a supervised machine learning model can then be used to predict the diversity of missing samples (conform Fig. 3). The use of predictive models can also be used to perform classification at the community level, to for example categorize communities according to the system they are part of (De Roy *et al.*, 2012; Dhoble *et al.*, 2018), or to identify a case versus control status.

Acknowledgements

The computational resources (Stevin Supercomputer Infrastructure) and services used in this work were provided by the VSC (Flemish Supercomputer Center), funded by Ghent University, the Hercules Foundation and the Flemish Government department EWI.

Funding

PR is supported by Ghent University (BOFSTA2015000501). RP is supported by Ghent University (BOFDOC2015000601).

References

Aghaeepour, N., Finak, G., Hoos, H., Mosmann, T. R., Brinkman, R., Gottardo, R., and Scheuermann, R. H. (2013). Critical assessment of automated flow cytometry data analysis techniques. *Nature Methods*, **10**(3), 228–238.

Amalfitano, S., Fazi, S., Ejarque, E., Freixa, A., Romaní, A. M., and Butturini, A. (2018). Deconvolution model to resolve cytometric microbial community patterns in flowing waters. *Cytometry Part A*, **93**(2), 194–200.

Ardui, S., Ameur, A., Vermeesch, J. R., and Hestand, M. S. (2018). Single molecule real-time (SMRT) sequencing comes of age: applications and utilities for medical diagnostics. *Nucleic Acids Research*, **46**(5), 2159–2168.

Barbesti, S., Citterio, S., Labra, M., Baroni, M. D., Neri, M. G., and Sgorbati, S. (2000). Two and three-color fluorescence flow cytometric analysis of immunoidentified viable bacteria. *Cytometry*, **40**(3), 214–218.

Bergstra, J. and Bengio, J. (2012). Random Search for Hyper-Parameter Optimization. *Journal of Machine Learning Research*, **13**, 281–305.

Besmer, M. D. and Hammes, F. (2016). Short-term microbial dynamics in a drinking water plant treating groundwater with occasional high microbial loads. *Water Research*, **107**, 11–18.

Bishop, C. M. (2006). *Pattern Recognition and Machine Learning*. Springer-Verlag, Berlin, Heidelberg.

Blaser, M. J., Cardon, Z. G., Cho, M. K., Dangl, J. L., Donohue, T. J., Green, J. L., Knight, R., Maxon, M. E., Northen, T. R., Pollard, K. S., and Brodie, E. L. (2016). Toward a Predictive Understanding of Earth ' s Microbiomes to Address 21st Century Challenges. *mBio*, **7**(3), 1–16.

Boedigheimer, M. J. and Ferbas, J. (2008). Mixture modeling approach to flow cytometry data. *Cytometry Part A*, **73**(5), 421–429.

Bray, J. R. and Curtis, J. T. (1957). An Ordination of the Upland Forest Communities of Southern Wisconsin. *Ecological Monographs*, **27**(4), 325–349.

Breiman, L. (2001). Random forests. *Machine learning*, **45**(1), 5–32.

Buysschaert, B., Byloos, B., Leys, N., Van Houdt, R., and Boon, N. (2016). Reevaluating multicolor flow cytometry to assess microbial viability. *Applied Microbiology and Biotechnology*, **100**, 9037–9051.

Chiang, E., Schmidt, M. L., Berry, M. A., Biddanda, B. A., Burtner, A., Johengen, T. H., Palladino, D., and Denef, V. J. (2018). Verrucomicrobia are prevalent in north- temperate freshwater lakes and display class- level preferences between lake habitats. *PLoS ONE*, **13**(3), 1–20.

Daly, A., Baetens, J., and De Baets, B. (2018). Ecological Diversity: Measuring the Unmeasurable. *Mathematics*, **6**(7), 119.

De Roy, K., Clement, L., Thas, O., Wang, Y., and Boon, N. (2012). Flow cytometry for fast microbial community fingerprinting. *Water Research*, **46**(3), 907–919.

De Vrieze, J., Boon, N., and Verstraete, W. (2018). Taking the technical microbiome into the next decade. *Environmental Microbiology*, **20**(6), 1991–2000.

Dhoble, A. S., Lahiri, P., and Bhalerao, K. D. (2018). Machine learning analysis of microbial flow cytometry data from nanoparticles , antibiotics and carbon sources perturbed anaerobic microbiomes. *Journal of Biological Engineering*, **12**(19), 1–15.

Falkowski, P. G., Fenchel, T., and Delong, E. F. (2008). The Microbial Engines That Drive Earth 's Biogeochemical Cycles. *Science*, **320**(5879), 1034–1039.

Friedman, J. and Alm, E. J. (2012). Inferring Correlation Networks from Genomic Survey Data. *PLoS Computational Biology*, **8**(9), 1–11.

García, F. C., Alonso-Sáez, L., Morán, X. A. G., and López-Urrutia, Á. (2015). Seasonality in molecular and cytometric diversity of marine bacterioplankton: The re-shuffling of bacterial taxa by vertical mixing. *Environmental Microbiology*, **17**(10), 4133–4142.

Gilbert, J. A. and Neufeld, J. D. (2014). Life in a World without Microbes. *PLoS Biology*, **12**(12), 1–3.

Günther, S., Koch, C., Hübschmann, T., Röske, I., Müller, R. A., Bley, T., Harms, H., and Müller, S. (2012). Correlation of community dynamics and process parameters as a tool for the prediction of the stability of wastewater treatment. *Environmental Science and Technology*, **46**(1), 84–92.

Günther, S., Becker, D., Hübschmann, T., Reinert, S., Kleinsteuber, S., Müller, S., and Wilhelm, C. (2018). Long-Term Biogas Production from Glycolate by Diverse and Highly Dynamic Communities. *Microorganisms*, **6**(4), 103.

Hammes, F., Broger, T., Weilenmann, H.-U., Vital, M., Helbing, J., Bosshart, U., Huber, P., Peter Odermatt, R., and Sonnleitner, B. (2012). Development and laboratory-scale testing of a fully automated online flow cytometer for drinking water analysis. *Cytometry Part A*, **81A**(6), 508–516.

Heyse, J., Buysschaert, B., Props, R., Rubbens, P., Skirtach, A. G., Waegeman, W., and Boon, N. (2019). Coculturing bacteria leads to reduced phenotypic heterogeneities. *Applied & Environmental Microbiology*.

Hill, M. O. (1973). Diversity and Evenness : A Unifying Notation and Its Consequences. *Ecology*, **54**(2), 427–432.

Huang, T. H., Tzeng, Y. L., and Dickson, R. M. (2018). FAST: Rapid determinations of antibiotic susceptibility phenotypes using label-free cytometry. *Cytometry Part A*, **93**(6), 639–648.

Hyrkas, J., Clayton, S., Ribalet, F., Halperin, D., Virginia Armbrust, E., and Howe, B. (2015). Scalable clustering algorithms for continuous environmental flow cytometry. *Bioinformatics*, **32**(3), 417–423.

Koch, C. and Müller, S. (2018). Personalized microbiome dynamics - Cytometric fingerprints for routine diagnostics. *Molecular Aspects of Medicine*, **59**, 123–134.

Koch, C., Fetzer, I., Harms, H., and Müller, S. (2013a). CHIC-an automated approach for the detection of dynamic variations in complex microbial communities. *Cytometry Part A*, **83 A**(6), 561–567.

Koch, C., Günther, S., Desta, A. F., Hübschmann, T., and Müller, S. (2013b). Cytometric fingerprinting for analyzing microbial intracommunity structure variation and identifying subcommunity function. *Nature protocols*, **8**(1), 190–202.

Koch, C., Harnisch, F., Schröder, U., and Müller, S. (2014). Cytometric fingerprints: Evaluation of new tools for analyzing microbial community dynamics. *Frontiers in Microbiology*, **5**(JUN), 1–12.

Konopka, A., Lindemann, S., and Fredrickson, J. (2015). Dynamics in microbial communities: Unraveling mechanisms to identify principles. *ISME Journal*, **9**(7), 1488–1495.

Leinster, T. and Cobbold, C. A. (2012). Measuring diversity: the importance of species similarity. *Ecology*, **93**(3), 477–489.

Li, W. K. W. (1997). Cytometric diversity in marine ultraphytoplankton. *Limnology and Oceanography*, **42**(5), 874–880.

Mantel, N. (1967). The Detection of Disease Clustering and a Generalized Regression Approach. *Cancer Research*, **27**(2), 209–220.

Menyhárt, L., Nagy, S., and Lepossa, A. (2018). Rapid analysis of photoautotroph microbial communities in soils by flow cytometric barcoding and fingerprinting. *Applied Soil Ecology*, **130**(June), 237–240.

Monaco, G., Chen, H., Poidinger, M., Chen, J., De Magalhães, J. P., and Larbi, A. (2016). FlowAI: Automatic and interactive anomaly discerning tools for flow cytometry data. *Bioinformatics*, **32**(16), 2473–2480.

Park, H. S., Schumacher, R., and Kilbane, J. J. (2005). New method to characterize microbial diversity using flow cytometry. *Journal of Industrial Microbiology and Biotechnology*, **32**(3), 94–102.

Pedregosa, F., Varoquaux, G., Gramfort, A., Michel, V., Thirion, B., Grisel, O., Blondel, M., Prettenhofer, P., Weiss, R., Dubourg, V., Vanderplas, J., Passos, A., Cournapeau, D., Brucher, M., Perrot, M., and Duchesnay, E. (2011). Scikit-learn: Machine Learning in Python. *Journal of Machien Learning Research*, **12**, 2825–2830.

Prest, E. I., Hammes, F., Kötzsch, S., van Loosdrecht, M. C. M., and Vrouwenvelder, J. S. (2013). Monitoring microbiological changes in drinking water systems using a fast and reproducible flow cytometric method. *Water Research*, **47**(19), 7131–7142.

Props, R., Monsieurs, P., Mysara, M., Clement, L., and Boon, N. (2016). Measuring the biodiversity of microbial communities by flow cytometry. *Methods in Ecology and Evolution*, **7**(11), 1376–1385.

Props, R., Schmidt, M. L., Heyse, J., Vanderploeg, H. A., Boon, N., and Denef, V. J. (2018). Flow cytometric monitoring of bacterioplankton phenotypic diversity predicts high population-specific feeding rates by invasive dreissenid mussels. *Environmental Microbiology*, **20**(2), 521–534.

Reiter, M., Rota, P., Kleber, F., Diem, M., Groeneveld-Krentz, S., and Dworzak, M. (2016). Clustering of cell populations in flow cytometry data using a combination of Gaussian mixtures. *Pattern Recognition*, **60**, 1029–1040.

Robinson, J. P. (2018). Overview of Flow Cytometry and Microbiology. *Current Protocols in Cytometry*, **84**(1), e37.

Rogers, W. T. and Holyst, H. A. (2009). FlowFP: A Bioconductor Package for Fingerprinting Flow Cytometric Data. *Advances in Bioinformatics*, **2009**(3), 1–11.

Rubbens, P., Props, R., Boon, N., and Waegeman, W. (2017a). Flow cytometric single-cell identification of populations in synthetic bacterial communities. *PLoS ONE*, **12**(1), e0169754.

Rubbens, P., Props, R., Garcia-Timermans, C., Boon, N., and Waegeman, W. (2017b). Stripping flow cytometry: How many detectors do we need for bacterial identification? *Cytometry Part A*, **91**(12), 1184–1191.

Rubbens, P., Schmidt, M. L., and Props, R. (2019). Randomized lasso associates freshwater lake-system specific bacterial taxa with heterotrophic production through flow cytometry. *bioRxiv*, (August), 1–42.

Scrucca, L., Fop, M., Murphy, T. B., and Raftery, A. E. (2016). mclust 5: Clustering, Classification and Density Estimation Using Gaussian Finite Mixture Models. *The R journal*, **8**(1), 289–317.

Sims, D., Sudbery, I., Ilott, N. E., Heger, A., and Ponting, C. P. (2014). Sequencing depth and coverage: Key considerations in genomic analyses. *Nature Reviews Genetics*, **15**(2), 121–132.

Stepanauskas, R., Fergusson, E. A., Brown, J., Poulton, N. J., Tupper, B., Labonté, J. M., Becraft, E. D., Brown, J. M., Pachiadaki, M. G., Povilaitis, T., Thompson, B. P., Mascena, C. J., Bellows, W. K., and Lubys, A. (2017). Improved genome recovery and integrated cell-size analyses of individual uncultured microbial cells and viral particles. *Nature Communications*, **8**(1), 1–10.

Tibshirani, R. (1996). Regression Selection and Shrinkage via the Lasso. *Journal of the Royal Statistical Society B*, **58**(1), 267–288.

Van Dijk, E., Auger, H., Jaszczyszyn, Y., and Thermes, C. (2014). Ten years of next-generation sequencing technology. *Trends in genetics*, **30**(9), 418–426.

van Dorst, J., Bissett, A., Palmer, A. S., Brown, M., Snape, I., Stark, J. S., Raymond, B., McKinlay, J., Ji, M., Winsley, T., and Ferrari, B. C. (2014). Community fingerprinting in a sequencing world. *FEMS Microbiology Ecology*, **89**(2), 316–330.

Van Nevel, S., Koetzsch, S., Weilenmann, H. U., Boon, N., and Hammes, F. (2013). Routine bacterial analysis with automated flow cytometry. *Journal of Microbiological Methods*, **94**(2), 73–76.

Vives-Rego, J., Resina, O., Comas, J., Loren, G., and Julià, O. (2003). Statistical analysis and biological interpretation of the flow cytometric heterogeneity observed in bacterial axenic cultures. *Journal of Microbiological Methods*, **53**(1), 43–50.

Weber, L. M. and Robinson, M. D. (2016). Comparison of clustering methods for high-dimensional single-cell flow and mass cytometry data. *Cytometry Part A*, **89**(12), 1084–1096.

Young, V. B. (2017). The role of the microbiome in human health and disease: An introduction for clinicians. *BMJ*, **356**.

Zimmermann, J., Hübschmann, T., Schattenberg, F., Schumann, J., Durek, P., Riedel, R., Friedrich, M., Glauben, R., Siegmund, B., Radbruch, A., Müller, S., and Chang, H. D. (2016). High-resolution microbiota flow cytometry reveals dynamic colitis-associated changes in fecal bacterial composition. *European Journal of Immunology*, **46**(5), 1300–1303.

Zou, H. and Hastie, T. (2005). Regularization and variable selection via the elastic net. *Journal of the Royal Statistical Society: Series B (Statistical Methodology)*, **67**(2), 301–320.